I&EC research
Industrial & Engineering Chemistry Research

Article

pubs.acs.org/IECR

Preparation of NiNbO/AISI 430 Ferritic Stainless Steel Monoliths for Catalytic Applications

J. A. Santander, E. López, G. M. Tonetto,* and M. N. Pedernera

PLAPIQUI (UNS-CONICET), Camino La Carrindanga Km. 7, Bahía Blanca, 8000 Argentina

ABSTRACT: AISI 430 ferritic stainless steel was used as a substrate to make catalytic monolithic structures. To increase the surface roughness of the substrate, the steel was oxidized at temperatures in the range of 900−940 °C and times in the range of 30−120 min. The oxide layer formed was characterized. Treatment at 940 °C for 60 min was found to be optimal for obtaining a Cr-rich rough oxide layer, with good adherence and homogeneity. Catalytic monoliths were prepared by dip-coating into four different slurries containing the Ni−Nb mixed oxide catalyst. The samples were characterized and tested in the oxidative dehydrogenation (ODH) of ethane to ethylene. The structured catalysts were active for the ODH of ethane, with very good selectivity to ethylene. The catalytic performance was remarkably constant for 170 h on stream at 400 °C.

1. INTRODUCTION

Ethane is the most abundant component of natural gas, apart from methane. The primary use of ethane is in the production of ethylene. Twenty-one percent of the current world production of ethylene is produced by the steam cracking of ethane, and the rest is mainly produced by the thermal cracking of petrochemical feedstocks such as naphtha, propane, and gas oil.[1]

The production of ethylene from ethane is carried out by thermal or catalytic dehydrogenation processes. However, the thermal process requires operation at high temperatures, with high energy costs and undesired side reactions. The catalytic conversion of ethane under oxidizing conditions is currently being studied as an energy-saving method for producing ethylene. Lower reaction temperatures and the absence of thermodynamic equilibrium limitations are some of the advantages offered by the catalytic oxidative dehydrogenation (ODH) of ethane.

A wide range of catalysts have been studied for the ODH of ethane. There are a great number of reports on the catalytic properties of vanadium oxide-based catalysts.[2] NiO-based catalysts also present a high performance in ethane ODH. In particular, Ni−Nb mixed oxides exhibit high activity and selectivity at low temperature, with ethylene yields above 40% at 400 °C.[3−6]

The use of these catalysts in conventional fixed-bed catalytic reactors could have some disadvantages, such as maldistributions resulting in nonuniform access of reactants to the catalytic surface, high pressure drops in the bed, and sensitivity to fouling by dust.[7]

Structured catalysts have been developed to avoid these issues. Monolithic catalysts are structures containing many narrow, parallel straight or zigzag passages, with the catalytic material deposited on the walls of the channels.

The typical support materials of monoliths are ceramics or metals. Metallic structures offer interesting advantages over ceramic monoliths, in terms of higher mechanical resistance and enhanced thermal conductivity. The possibility of using thinner walls leading to higher cell density and lower pressure drop is also reported.[8]

However, the use of metals as substrates for the deposition of catalytic layers requires a pretreatment to improve the adherence of the active material to the metallic surface.

A number of studies have been reported on the use of Fecralloy, which generates a layer of alumina whiskers on the surface after thermal treatments.[9,10] Thermal treatments are also used for stainless steels. Austenitic stainless steels such as AISI 304 develop a rough oxide layer at high temperature, and the duration and temperature level of the treatment have a strong influence on the morphology, integrity, and homogeneity of the formed layer.[11] Metal foams made of AISI 316[12] and AISI 314[13] stainless steels have also been used as substrates on which to deposit catalytic coatings.

Ferritic stainless steel is an attractive alternative to the typically employed austenitic stainless steel because of its strength, ductility, and corrosion resistance.[14] AISI 430 ferritic stainless steel is used in a large number of applications, but to our knowledge, there are no reports on its use as a monolithic substrate in structured reactors. This alloy is an interesting material for the production of metallic monoliths because it is not expensive and is available in thin layers and because it has suitable mechanical properties for this purpose.

Bortolozzi et al.[15] studied the ODH of ethane over structured reactors with Ni and Ni−Ce/Al_2O_3 catalysts, using stainless steel foams as substrates. The catalysts were active and selective for this reaction at low temperatures (300−450 °C). The ODH reaction was also studied on a $LaMnO_3$-based monolith,[16] V_2O_5/TiO_2-coated stainless steel foam and plates,[17,18] and MoVTeNbO supported on SiC foam.[19]

The present contribution reports studies concerning the determination of appropriate conditions for the thermal pretreatment of the surface of AISI 430 ferritic stainless steel monoliths in an oxygen atmosphere to produce a rough, homogeneous, and well-adhered oxide film over these

Received: May 7, 2014
Revised: June 16, 2014
Accepted: June 17, 2014

dx.doi.org/10.1021/ie501884g | *Ind. Eng. Chem. Res.* XXXX, XXX, XXX−XXX

structured substrates. Results regarding the coating of the substrates by washcoating with an active and selective Ni−Nb mixed oxide catalysts are also reported here. Finally, the prepared monolithic catalyst was tested in the ODH of ethane to ethylene.

2. EXPERIMENTAL SECTION

2.1. Preparation of the Structured Substrates. For the preparation of the monoliths, 100-μm-thick AISI 430 stainless steel foils (supplied by ACZ INOX) were used. The composition of the steel is reported in Table 1.

Table 1. Composition of the AISI 430 Ferritic Stainless Steel by Weight[a]

element	content (wt %)	element	content (wt %)
C	0.08 ± 0.01	P	0.040 ± 0.005
Si	1.00 ± 0.05	S	0.030 ± 0.005
Mn	1.00 ± 0.03	Cr	16.0−18.0 ± 0.2

[a]Fe balance.

Steel foils (28.2 cm length by 3 cm width) were washed with detergent several times and rinsed with distilled water. Then, they were dried in a stove at 120 °C for 60 min and cleaned with acetone to remove any remaining organic impurity. The monoliths were made by rolling flat and corrugated foils, with multiple parallel channels of equal geometry. Thus, cylindrical monoliths of 1.5-cm diameter and 3-cm length were obtained, with a surface area of 169 cm^2 and a cell density of 65 cells/cm^2.

To generate a rough surface adequate for the subsequent deposition of the catalytic film, the metallic monoliths were subjected to different thermal treatments. These treatments consisted of calcining the samples in a horizontal oven at different temperatures (900−940 °C) and for different oxidation times (30−120 min) in the presence of an analytic air flow (Air Liquide). The heating rate was 13 °C/min. After the treatment, the samples were cooled at room temperature under the same atmosphere.

2.2. Preparation of the Powder Catalyst. The Ni−Nb mixed oxide was prepared with a Ni/Nb molar ratio of 0.85/0.15. The powder catalyst was obtained by the evaporation method. First, an aqueous solution of nickel(II) nitrate hexahydrate (Aldrich, 99.999% purity) and ammonium niobate-(V) oxalate hydrate (Aldrich, 99.99% purity) was prepared. Then, the solvent was evaporated at 70 °C under continuous agitation and dried at 120 °C for 12 h. The resulting material was calcined at 450 °C for 5 h. The powder catalyst obtained is denoted as NiNbO.

2.3. Preparation of the Structured Reactor. The structured substrates were coated with the catalyst by the dip-coating method. For that purpose, aqueous suspensions with 10, 15, and 30 wt % of the active phase were prepared. In all cases, 10% colloidal SiO_2 (Ludox TMA, Aldrich) was added as a stabilizer. Poly(vinyl alcohol) (PVA) was added in a proportion of 2−3% to increase the suspension viscosity and control the drying rate, helping to decrease the number of cracks.[20]

The substrate was immersed in the suspension at a rate of 3 cm/min, and the excess material was removed by centrifugation (550 rpm for 3 min). Then, it was dried at 80 °C for 30 min. The procedure was repeated until the desired catalyst loading on the monolith was obtained (~250 mg), and finally, the sample was calcined at 450 °C for 2 h in air.

The 30 wt % catalyst suspension that was not employed in the coating was dried and calcined to obtain a powder and to study this powder in reaction and compare the performance with that of the monolithic catalysts. The powder is denoted as CS-30.

2.4. Characterization. The morphology of the surface of the substrate was examined by scanning electron microscopy (SEM) on a JEOL JSM 35CF microscope.

The Cr/Fe ratio (w/w) of the samples was determined by energy-dispersive X-ray (EDX) analysis in an EDAX DX-4 microanalyzer. The X-ray diffraction patterns were obtained using a Philips PW1710 diffractometer, with a copper anode with a curved graphite monochromator, operated at 45 kV and 30 mA, with Cu Kα radiation, in the 2θ range between 5° and 70° at an interval of 0.0358°.

Roughness measurements were determined using a Mitutoyo SJ-201 surface roughness tester.

The adherence of the oxide layer formed on the metallic substrate after the thermal treatment and the adherence of the catalytic layer obtained by the dip-coating method were both tested by the ultrasonic method. The monoliths were immersed in 30 mL of diethyl ether and subjected to an ultrasonic bath for 30 min in a Cole Parmer 8892E-MT (47 kHz, 105 W) instrument at room temperature. Then, the solvent was evaporated. The weight of each monolith was measured before and after the ultrasonic treatment to determine the adherence, which was calculated as the percentage ratio of the amount of oxide retained to the amount of oxide present before the treatment.

The metal content (Ni and Nb) was determined by inductively coupled plasma (ICP) analysis. Specific surface areas were determined by N_2 adsorption at 77 K, using the multipoint Brunauer−Emmett−Teller (BET) analysis method with a Quantachrome NOVA 1200e apparatus.

The viscosity of the suspensions was measured with an Anton Paar Physica MCR 301 rheometer.

2.5. Catalytic Tests. The evaluation of the monoliths in the ODH of ethane was performed using a stainless steel tube of 16-mm inside diameter and 70-mm length into which the monoliths were placed. The calcined catalytic suspension (CS-30) tests were performed in a fixed-bed reactor using a 4.2-mm-internal-diameter glass tube. The tests were carried out at atmospheric pressure and at reaction temperatures varying between 300 and 400 °C. The feedstock consisted of an O_2/C_2H_6/He mixture with a 5/5/90 molar ratio. The flow rate was fixed to achieve a catalyst weight to flow ratio (W/F) equal to 0.54 g·s/cm^3. The reaction products were analyzed with an HP Agilent 4890D gas chromatograph equipped with a thermal conductivity detector. Two columns were used in the analysis: Porapak QS and Molecular Sieve 5 Å.

3. RESULTS AND DISCUSSION

3.1. Preparation of the Monolithic Substrate. The AISI 430 ferritic stainless steel was calcined to obtain an adequate surface for depositing the catalyst. Measurements of surface roughness, adherence, and Cr/Fe weight ratio by weight for the different treatment times and temperatures are also presented in panels A and B, respectively, of Figure 1. As shown, the weights increased as the temperature level and treatment time increased. This increment is due to the formation of a Cr-rich oxide film on the metallic substrate. As mentioned above, the main components of AISI 430 ferritic stainless steel are Fe and Cr (Table 1). The formation of Cr_2O_3 from Cr is an

dx.doi.org/10.1021/ie501884g | Ind. Eng. Chem. Res. XXXX, XXX, XXX−XXX

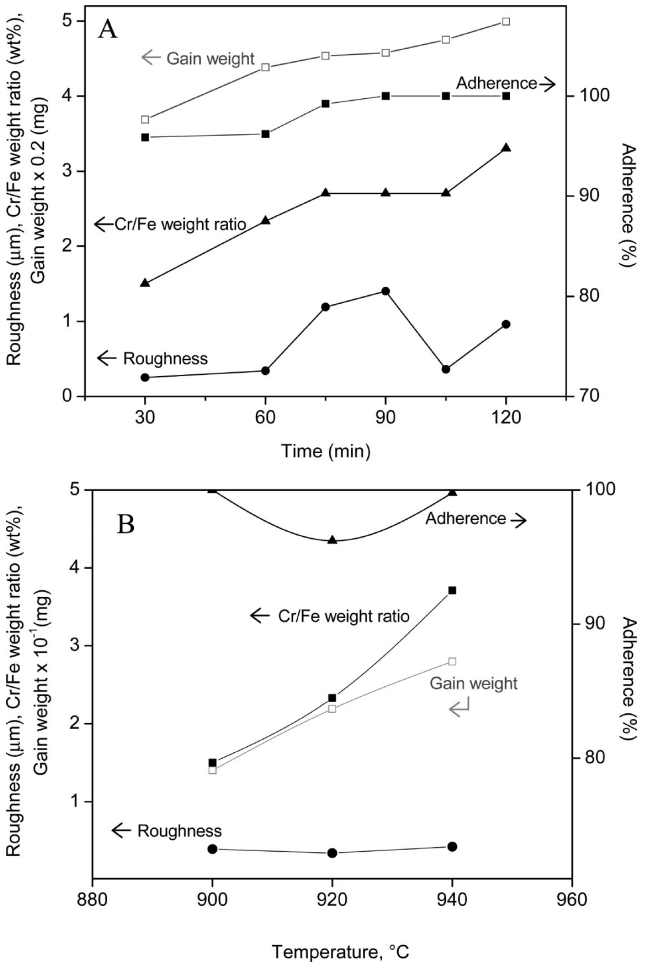

Figure 1. Variation of the properties of the oxide layer formed (A) at 920 °C at different treatment times and (B) at 60 min at different treatment temperatures.

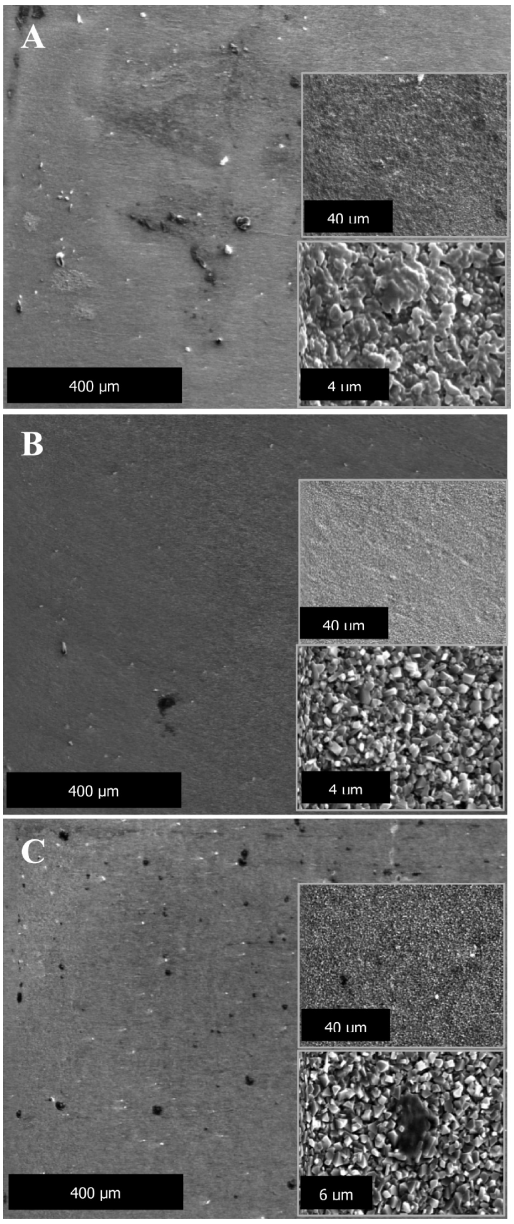

Figure 2. SEM images of the oxide layer formed on the AISI 430 ferritic steel after thermal treatments at 920 °C for (A) 30, (B) 60, and (C) 90 min.

energetically more favorable process than the oxidation of Fe, and therefore, Cr_2O_3 is the most stable oxide. At temperatures such as those used in the thermal treatment, Cr has sufficient mobility to segregate to the surface and combine with oxygen.[21]

The amount of oxide generated increased with increasing treatment time at constant temperature. In fact, at 920 °C, the weight of the metallic substrate for the 120-min thermal treatment was 35% larger than that obtained at 30 min. Up to 90 min, the curve of weight gain presents the typical parabolic behavior of high-temperature oxidation of this type of alloy.[22−24] The linear increase at longer times corresponds to the mechanism of breakaway corrosion, usually attributed to mechanical failure of the chromia scale.[25]

For a constant oxidation time, the increase in temperature generated a larger amount of oxide (Figure 1B). Temperature affects the mobility of the components of the alloy, making them available at the surface to react with the oxygen.

It can be observed in Figure 1A that the concentration of Cr on the surface increased with calcination time, indicating the preferential oxidation of Cr over Fe. The enrichment of Cr at the surface was evident in all cases. The Cr/Fe weight ratio at the surface of the oxidized substrates was between 7 and 16 times higher than that of the untreated alloy (the Cr/Fe weight ratio for the untreated alloy was ∼0.19).

For the treatments at a constant temperature of 920 °C, the maximum surface roughness was observed at an exposure time of 90 min (Figure 1A), whereas the adherence increases to ∼75 min and then remains almost constant.

When calcination temperature increased for an exposure time of 60 min, the amount of oxide formed and the surface concentration of Cr increased, as shown in Figure 1B. As mentioned, the increase observed in surface Cr content is the result of an increase in Cr mobility.

For the different temperature levels studied, no significant variations in surface roughness were observed, whereas adherence presented a minimum value at 920 °C.

The characteristics of the surface morphology of the substrates presented in Figure 1 are shown in SEM micrographs in Figures 2 and 3.

When the treatment time was longer than 75 min, at a constant temperature of 920 °C, the formation of blisters on the oxide layer was detected. The blisters were produced during

dx.doi.org/10.1021/ie501884g | Ind. Eng. Chem. Res. XXXX, XXX, XXX−XXX

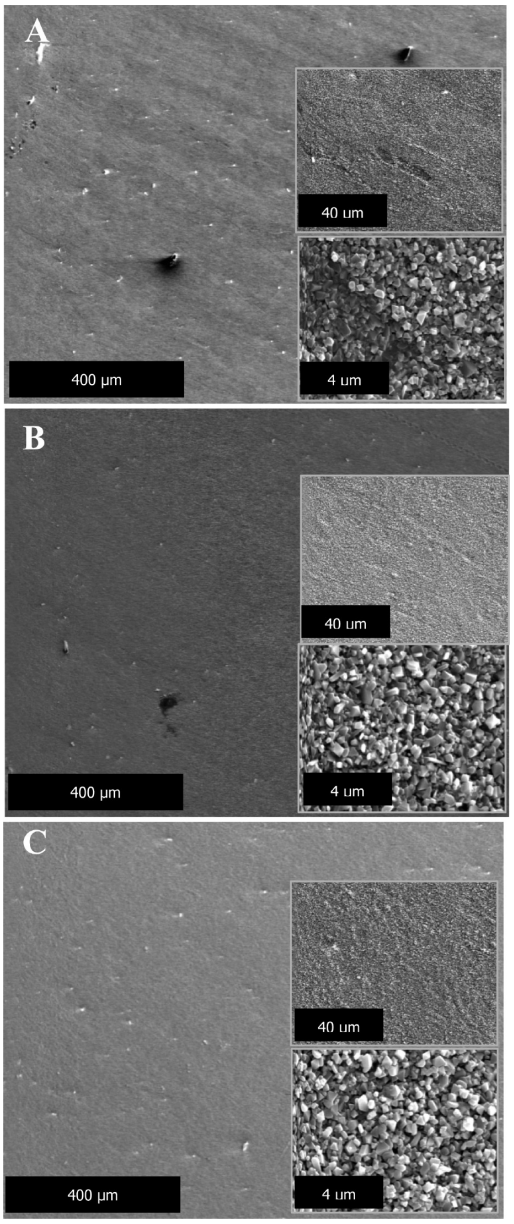

Figure 3. SEM images of the oxide layer formed on the AISI 430 ferritic steel after thermal treatments for 60 min at (A) 900, (B) 920, and (C) 940 °C.

cooling as a result of the different thermal expansion coefficients between the oxide scale and the base metal.[11]

As shown in the SEM micrographs, the substrates developed randomly oriented crystals on their surfaces under different oxidative treatments. According to published reports, when AISI 430 steels are treated under oxidative conditions at high temperature, they develop surface crystals corresponding to spinels that contain Cr, Fe, and Mn, and below this spinel layer, Cr_2O_3 is formed.[23,26] The results obtained at different times indicate that the most appropriate treatment was that of 60 min, because the surface presented the highest homogeneity.

The best surface characteristics observed in the oxide layer by SEM corresponded to the treatment at 940 °C (Figure 3). At this calcination temperature, although no significant increase in roughness was observed, a very good adherence of the oxide layer was recorded (99.8%), resulting in an adequate surface for depositing the catalytic film. Based on these results, it was

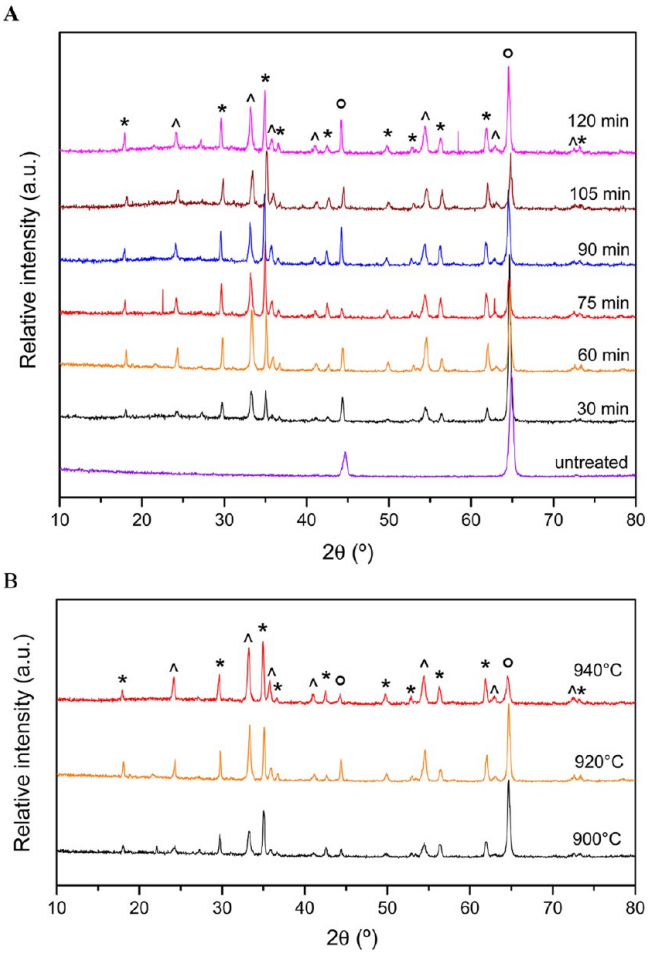

Figure 4. XRD patterns for AISI 430 at (A) varying treatment time at 920 °C and (B) varying treatment temperature at a constant time of 60 min. Reference: *, (Cr,Fe, and/or Mn)$_3$O$_4$ spinels; ∧, Cr_2O_3; ○, base alloy.

Table 2. Compositions and Viscosities of the Catalytic Suspensions Used for Washcoating

slurry	catalyst (wt %)	colloidal silica (wt %)	PVA (wt %)	viscosity[a] (mPa·s)
I	10	10	3	20
II	15	10	3	25
III	30	10	2	28
IV	30	10	0	9[b]

[a]Measured at a deformation rate of 2500 s^{-1}. [b]This sample presented a different rheological behavior.

decided to prepare the substrate of the monolithic catalyst by thermally treating AISI 430 ferritic stainless steel at 940 °C for 60 min. As discussed below, the roughness developed on the substrate by this treatment were sufficient to achieve high adherence of the catalytic layer.

X-ray diffractograms of the AISI 430 steel thermally treated at 900 °C for different times are presented in Figure 4A. For the untreated sample, two signals were observed at 2θ 44.7° and 64.9°, which are characteristic of this ferritic alloy. The treated samples presented signals that correspond to (Cr,Fe, and/or Mn)$_3$O$_4$ spinels, Cr_2O_3, and the base alloy.[26] In the steel treated for 30 min, the signals of this chemical species presented lower intensities compared to those observed for the rest of the samples. This indicates a lower formation of these

dx.doi.org/10.1021/ie501884g | Ind. Eng. Chem. Res. XXXX, XXX, XXX−XXX

Table 3. Properties of the Monoliths and the Calcined Catalytic Suspension (CS-30)

monolith	catalyst loading (mg/monolith)	number of coatings	adherence (%)	S_{BET} (m^2/g_{WC})	pore volume (cm^3/g_{WC})	pore radius (Å)
M15	305	10	99	74	0.209	56.6
M30	338	2	87	70	0.204	57.8
M30noPVA	280	2	92	63	0.206	65.6
CS-30	–	–	–	61	0.195	63.7

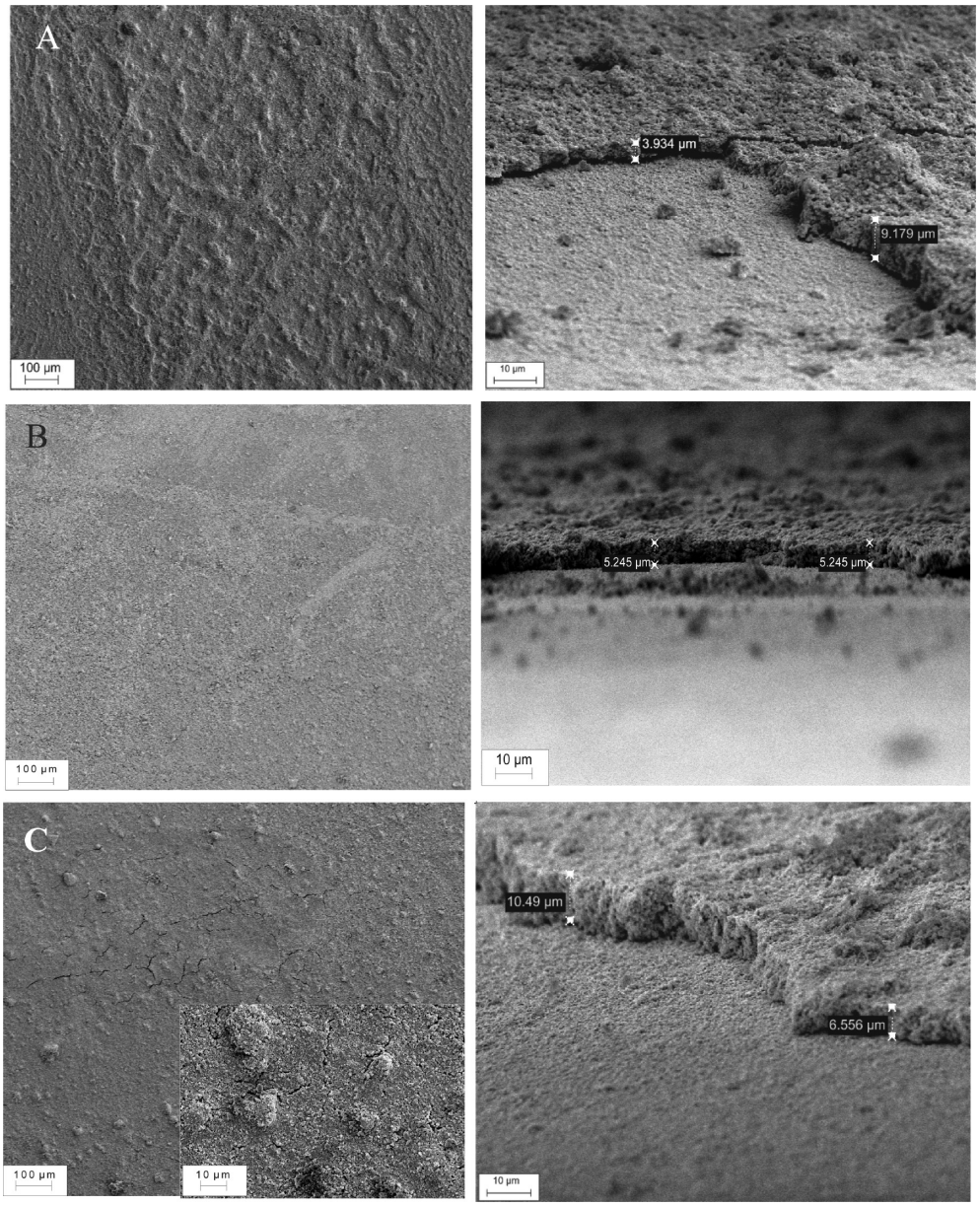

Figure 5. SEM images of the surfaces of monoliths and cross section of the catalytic layer for (A) M15, (B) M30, and (C) M30noPVA.

oxides because of the short exposure time, which is in agreement with the lower weight increase for this treatment time (Figure 1A). For the rest of the times, the intensities remained approximately constant. When the samples treated at different temperatures for 60 min were analyzed (Figure 4B), the same signals corresponding to (Cr,Fe, and/or Mn)$_3O_4$ spinels, Cr_2O_3, and the base alloy were found, but it is notable that, whereas the peaks corresponding to the oxides increased with temperature, the intensities of the untreated sample decreased.

The stability of the monolithic substrate (940 °C, 60 min) was studied for 30 h under conditions similar to those to which it was exposed during catalytic tests. To perform a conservative analysis, a higher reaction temperature (400 °C) and oxygen concentration (21%) were analyzed. No changes in the amount of surface oxide or monolith adherence were observed (results not shown).

3.2. Catalytic Suspension. *3.2.1. Suspension and Catalytic Coating.* The compositions of the aqueous suspensions prepared to coat the substrates are listed in Table 2. Colloidal SiO_2 was added to the mixtures to stabilize

dx.doi.org/10.1021/ie501884g | Ind. Eng. Chem. Res. XXXX, XXX, XXX–XXX

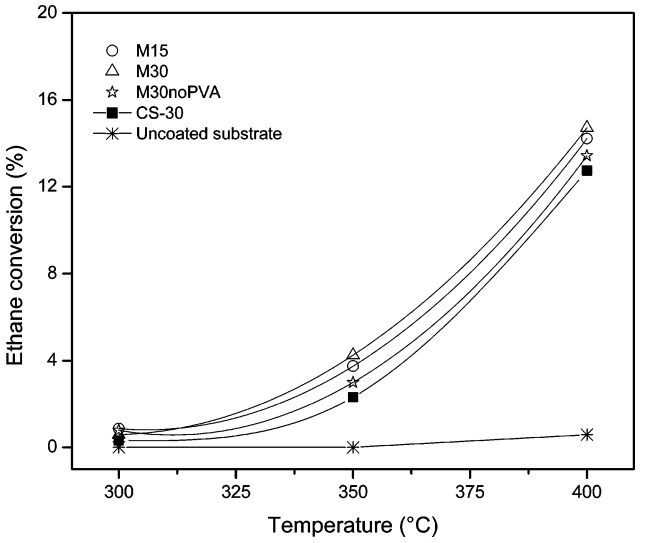

Figure 6. Ethane conversion as a function of temperature in the ODH of ethane (operating conditions: $O_2/C_2H_6/He$ = 5/5/90, W/F = 0.54 g·s/cm^3).

Table 4. Reactant Conversions and Product Selectivities[a]

	conversion (%)		selectivity (%)	
sample	C_2H_6	O_2	C_2H_4	CO_2
M15	14.2	17.3	63.6	36.4
M30	14.7	19.3	62.6	37.4
CS-30	14.7	15.5	75.8	24.2
uncoated monolith	0.6	1.0	0.0	100

[a]Operating conditions: $O_2/C_2H_6/He$ = 5/5/90, T = 400°C.

the suspensions and improve the adherence of the catalyst particles to the surface of the substrate. The PVA added had a double effect, modifying the viscosity of the catalytic suspension and controlling the drying rate, decreasing the number of cracks.[20] The adherence of the catalytic material to the substrate strongly depends on the particle size of the powder to be deposited. The catalyst used for the preparation of the suspensions had a diameter d_{90} equal to 3.04 μm (90% of the particles of the sample had a diameter of less than 3.04 μm), which was within the range suggested by the literature to obtain an adequate adherence.[27] The NiNbO catalyst had a specific area of 81 m^2/g and a pore volume of 0.182 cm^3/g.

As observed in Table 2, the viscosity of the suspensions increased with the amount of catalyst when PVA was present. The suspension with 10% catalyst presented a relatively low viscosity value. No washcoatings were performed at this concentration level because the number of immersions necessary to reach the desired loading would have been excessive. In the case of suspension IV, a different behavior was observed at high deformation rates, presenting a lower viscosity than the rest. However, the washcoating could be performed satisfactorily because, at low deformation rates, the behavior of the fluid was very similar to that of suspension III. This difference was attributed to the high content of solids without the thickening additive of the suspension, such as PVA.

The net loading of NiNbO catalyst deposited was approximately 250 mg per monolith. The properties of the prepared monoliths are detailed in Table 3. The monoliths are labeled according to the catalyst loading used in the suspension.

Table 3 shows that the best adherence was obtained for monolith M15, prepared with suspension II. This high level of adherence could be associated with the lower loading by immersion (which generated thin catalyst layers) and with the higher silica/catalyst ratio compared to M30 and M30noPVA. The silica added to the preparation remained in the coating after calcination, acting as a ligand of the catalyst particles.[10] The morphological properties of the prepared samples exhibited no significant difference (Table 3).

The catalytic layer obtained after successive immersions presented good homogeneity, especially for monolith M30 (Figure 5B). Cracks were observed on the surface of the M30noPVA sample (Figure 5C), which could be explained by the absence of PVA. However, this had no adverse effect on adherence (Table 3). The thickness of the coating on the substrates varied between 3 and 11 μm (Figure 5A–C).

3.2.2. Catalytic Activity. The monoliths coated with the catalytic material were studied in the ODH of ethane. The ethane conversions obtained with the monolithic catalysts at reaction temperatures in the 300–400 °C range are shown in Figure 6, along with the activity of CS-30, evaluated in a fixed-bed reactor. The feed flow rate was adjusted considering the amount of the active phase (NiNbO) deposited on each monolith and present in the calcined suspension CS-30, to maintain the same W/F ratio (0.54 g·s/cm^3). Preliminary calculations indicated the absence of internal mass-transfer limitations for the particles of CS-30 or the catalytic coatings of the three monoliths studied.

The ethane conversion observed for the different monolithic catalysts did not present significant differences in the temperature range studied. This is mainly because of the similar specific areas, coating thicknesses, and catalyst/flow ratios used in the tests. At 400 °C, conversion was within the 13.4–14.7% range.

When compared with the calcined catalytic suspension CS-30, the monoliths presented slightly higher values for ethane conversion (at 400 °C, it was 5–15% higher). This difference could be attributed to the effect of the presence of steel

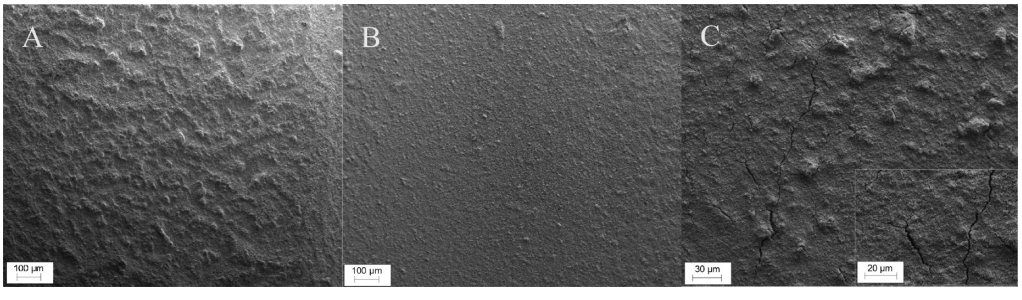

Figure 7. SEM images of the surfaces of monoliths after reaction for (A) M15, (B) M30, and (C) M30noPVA.

dx.doi.org/10.1021/ie501884g | Ind. Eng. Chem. Res. XXXX, XXX, XXX–XXX

(monolithic substrate and metallic reactor) exposed to the reactants and/or the different fluid dynamics of the reaction systems used (fixed bed vs monolithic reactor).

To analyze the effect of the steel, tests were carried out with an empty reactor and an uncoated monolithic substrate. A conversion of 0.7% was observed in the first case and 1.3% in the second case, showing that the substrate and the reactor were not inert. This could contribute to the conversion increase. The contribution to the catalytic activity by chromium species present in the oxide film of monolithic substrates has been previously reported.[15]

Selectivities toward ethylene at 400 °C for the monoliths, the calcined catalytic suspension, and the uncoated monolith are presented in Table 4. Catalytic tests were performed at varying W/F ratio to obtain equal ethane conversion levels, except for the uncoated monolith, which presented a very low activity. It can be noted that only ethylene and carbon dioxide were observed as reaction products. Selectivities toward ethylene of ∼63% and 76% were measured for the monoliths and CS-30 sample, respectively. This difference could again be attributed to the catalytic activities of the reactor and the uncoated metallic substrate (due to the presence of imperfections in the catalytic layer), which in previous tests showed complete selectivity to CO_2.

Figure 7 shows SEM images of the surfaces of the monoliths after 6 h of reaction. The similarity with the fresh samples previously shown in Figure 5 can be noted. A homogeneous coating is observed for all three spent monoliths, with good adherence. The cracks in Figure 7C for the M30noPVA sample were already present before the reaction, and the catalytic test did not increase their formation.

The stability of the catalytic performance of the monoliths was evaluated by performing a reaction test for 170 h at 400 °C. No changes in activity or selectivity were observed.

4. CONCLUSIONS

The results obtained in the present work showed the feasibility of using AISI 430 ferritic stainless steel as a substrate in the preparation of monolithic structures. By oxidation treatment under a controlled atmosphere at 940 °C for 60 min, a rough surface oxide layer was obtained, with good adherence and homogeneity, suitable for the subsequent deposition of the catalyst.

Stable catalytic suspensions of Ni−Nb mixed oxide were prepared, using adequate values of particle size, concentration of solids, and additives.

It was possible to obtain monolithic catalysts with a homogeneous coating, good adherence, and the desired active phase loading by means of the dip-coating technique.

The structured catalysts were active in the ODH of ethane, with very good selectivity toward ethylene. The catalytic performance was remarkably constant for 170 h on stream at 400 °C.

AUTHOR INFORMATION

Corresponding Author

*Tel.: +54 291 4861700. Fax: +54 291 4861600. E-mail: gtonetto@plapiqui.edu.ar.

Notes

The authors declare no competing financial interest.

ACKNOWLEDGMENTS

The authors thank Ing. D. Ziegler and Ing. P. Benedetti for their assistance with the roughness measurements (Engineering Department, UNS) and the Universidad Nacional del Sur (UNS), the Consejo Nacional de Investigaciones Científicas y Técnicas (CONICET), and the Agencia Nacional de Promoción Científica y Tecnológica (ANPCyT) for financial support.

REFERENCES

(1) Neelis, M.; Patel, M.; Blok, K.; Haije, W.; Bach, P. Approximation of theoretical energy-saving potentials for the petrochemical industry using energy balances for 68 key processes. *Energy* **2007**, *32*, 1104.

(2) Cavani, F.; Ballarini, N.; Cericola, A. Oxidative dehydrogenation of ethane and propane: How far from commercial implementation? *Catal. Today* **2007**, *127*, 113.

(3) Heracleous, E.; Lemonidou, A. A. Ni−Nb−O mixed oxides as highly active and selective catalysts for ethene production via ethane oxidative dehydrogenation. Part I: Characterization and catalytic performance. *J. Catal.* **2006**, *237*, 162.

(4) Savova, B.; Loridant, S.; Filkova, D.; Millet, J. M. M. Ni−Nb−O catalysts for ethane oxidative dehydrogenation. *Appl. Catal. A* **2010**, *390*, 148.

(5) Zhu, H.; Ould-Chikh, S.; Anjum, D. H.; Sun, M.; Biausque, G.; Basset, J.; Caps, V. Nb effect in the nickel oxide-catalyzed low-temperature oxidative dehydrogenation of ethane. *J. Catal.* **2012**, *285*, 292.

(6) Heracleous, E.; Delimitis, A.; Nalbandian, L.; Lemonidou, A. A. HRTEM characterization of the nanostructural features formed in highly active Ni−Nb−O catalysts for ethane ODH. *Appl. Catal. A* **2007**, *325*, 220.

(7) Cybulski, A.; Moulijn, J. *Structured Catalysts and Reactors*; Marcel Dekker: New York, 1998.

(8) Avila, P.; Montes, M.; Miro, E. E. Monolithic reactors for environmental applications. A review on preparation technologies. *Chem. Eng. J.* **2005**, *109*, 11.

(9) Pérez, H.; Navarro, P.; Montes, M. Deposition of SBA-15 layers on Fecralloy monoliths by washcoating. *Chem. Eng. J.* **2010**, *158*, 325.

(10) Eleta, A.; Navarro, P.; Costa, L.; Montes, M. Deposition of zeolitic coatings onto Fecralloy microchannels: Washcoating vs. in situ growing. *Microporous Mesoporous Mater.* **2009**, *123*, 113.

(11) Martínez Tejada, L. M.; Sanz, O.; Domínguez, M.; Centeno, M.; Odriozola, J. AISI 304 Austenitic stainless steels monoliths for catalytic applications. *Chem. Eng. J.* **2009**, *148*, 191.

(12) Sang, L.; Sun, B.; Tan, H.; Du, C.; Wu, Y.; Ma, C. Catalytic reforming of methane with CO_2 over metal foam based monolithic catalysts. *Int. J. Hydrogen Energy* **2012**, *37*, 13037.

(13) Bortolozzi, J. P.; Gutierrez, L. B.; Ulla, M. A. Synthesis of Ni/Al_2O_3 and Ni−Co/Al_2O_3 coatings onto AISI 314 foams and their catalytic application for the oxidative dehydrogenation of ethane. *Appl. Catal. A* **2013**, *452*, 179.

(14) Amuda, M. O. H.; Mridha, S. Microstructural features of AISI 430 ferritic stainless steel (FSS) weld produced under varying process parameters. *Int. J. Mech. Mater. Eng.* **2009**, *4*, 160.

(15) Bortolozzi, J. P.; Weiss, T.; Gutierrez, L. B.; Ulla, M. A. Comparison of Ni and Ni−Ce/Al_2O_3 catalysts in granulated and structured forms: Their possible use in the oxidative dehydrogenation of ethane reaction. *Chem. Eng. J.* **2014**, *246*, 343.

(16) Donsi, F.; Pirone, R.; Russo, G. Oxidative dehydrogenation of ethane over a perovskite-based monolithic reactor. *J. Catal.* **2002**, *209*, 51.

(17) Giornelli, T.; Lofberg, A.; Guillou, L.; Paul, S.; Le Courtois, V.; Bordes-Richard, E. Catalytic wall reactor: Catalytic coatings of stainless steel by VO_x/TiO_2 and Co/SiO_2 catalysts. *Catal. Today* **2007**, *128*, 201.

(18) Löfberg, A.; Essakhi, A.; Paul, S.; Swesi, Y.; Zanota, M. L.; Meille, V.; Pitault, I.; Supiot, P.; Mutel, B.; Le Courtois, V.; Bordes-Richard, E. Use of catalytic oxidation and dehydrogenation of

hydrocarbons reactions to highlight improvement of heat transfer in catalytic metallic foams. *Chem. Eng. J.* **2011**, *176*−*177*, 49.
(19) Nguyen, T. T.; Burel, L.; Nguyen, D. L.; Pham-Huu, C.; Millet, J. M. M. Catalytic performance of MoVTeNbO catalyst supported on SiC foam in oxidative dehydrogenation of ethane and ammoxidation of propane. *Appl. Catal. A* **2012**, *433*−*434*, 41.
(20) Agrafiotis, C.; Tsetsekou, A. Deposition of meso-porous γ-alumina coatings on ceramic honeycombs by sol−gel methods. *J. Eur. Ceram. Soc.* **2002**, *22*, 423.
(21) Greyling, C. J.; Roux, J. P. Optimum conditions in the thermal passivation of aisi 430 and 304 stainless steel in controlled oxygen atmosphere. *Corros. Sci.* **1984**, *24*, 675.
(22) Hay, K. A.; Hicks, F. G.; Holmes, D. R. The Transport Properties and Defect Structure of the Oxide $(Fe,Cr)_2O_3$ formed on Fe−Cr alloys. *Mater. Corros.* **1970**, *21*, 917.
(23) Ebrahimifar, H.; Zandrahimi, M. Study of parabolic rate constant for coated AISI 430 steel with Mn_3O_4 and $MnFe_2O_4$ spinels. *Indian J. Eng. Mater. Sci.* **2011**, *18*, 314.
(24) Ishiguro, K.; Homma, T. Thin oxide films on a ferritic and an austenitic alloy. In *International Corrosion Conference*; NACE International: Houston, TX, 1981; p 28.
(25) Shreir, L. L. *Corrosion Vol. 1: Metal/Environment Reactions*; Butterworth-Heinemann: Oxford, U.K., 1976.
(26) Rufner, J.; Gannon, P.; White, P.; Deibert, M.; Teintze, S.; Smith, R.; Chen, H. Oxidation behavior of stainless steel 430 and 441 at 800 °C in single (air/air) and dual atmosphere (air/hydrogen) exposures. *Int. J. Hydrogen Energy* **2008**, *33*, 1392.
(27) Agrafiotis, C.; Tsetsekou, A. The effect of powder characteristics on washcoat quality. Part I: Alumina washcoats. *J. Eur. Ceram. Soc.* **2000**, *20*, 815.